

Coupling Time-Domain Analysis for Dynamic Positioning during S-Lay Installation

Sun Li-ping, Zhu Jian-xun, Liu Sheng-nan

Abstract—In order to study the performance of dynamic positioning system during S-lay operations, dynamic positioning system is simulated with the hull-stinger-pipe coupling effect. The roller of stinger is simulated by the generalized elastic contact theory. The stinger is composed of Morrison members. Force on pipe is calculated by lumped mass method. Time domain of fully coupled barge model is analyzed combining with PID controller, Kalman filter and allocation of thrust using Sequential Quadratic Programming method. It is also analyzed that the effect of hull wave frequency motion on pipe-stinger coupling force and dynamic positioning system. Besides, it is studied that how S-lay operations affect the dynamic positioning accuracy. The simulation results are proved to be available by checking pipe stress with API criterion. The effect of heave and yaw motion cannot be ignored on hull-stinger-pipe coupling force and dynamic positioning system. It is important to decrease the barge's pitch motion and lay pipe in head sea in order to improve safety of the S-lay installation and dynamic positioning.

Keywords—S-lay operation, dynamic positioning, coupling motion; time domain, allocation of thrust.

I. INTRODUCTION

A Dynamic Positioning System (DPS) is an essential requirement for marine vessels and in many offshore platform operations, especially in deepwater production units, for keeping desired position and heading. DPS mainly consist of three primary units: sensors unit, control and monitoring unit, and the actuators unit. The information from sensors, including the position and heading and wind, is processed in the control and monitoring unit which produces the required control signals to the actuators unit. And then the actuators unit develops the required thrust and direction for each actuator among the thrusters' configuration with respect to the surge and sway axis [1].

Since the first presence of the DP system in 1960s, it has been widely used in the marine sector, oil and gas industries, and military services such as drilling, pipe-laying, anchor handling, docking and towing, search and rescue etc. Ayman B. Mahfouz [2] presented a new software program capable of estimating the environmental forces, thrusters' capability calculations, and capability polar plots for a marine vessel. Haibo Chen [3], [4] analyzed the dynamic positioning of mobile offshore drilling units for drilling operation and the collision between a DP shuttle tanker and FPSO. Pettersen et al.

Sun Li-ping is with the Deepwater Engineering Research Center, Harbin Engineering University, Harbin, China (phone: 86-451-82569359; fax: 86-451-82518398; e-mail: hualshu2@163.com).

Zhu Jian-xun and Liu Sheng-nan are with the Deepwater Engineering Research Center, Harbin Engineering University, Harbin, China (e-mail: hualshu2@163.com, hualshu2@163.com).

[5] addressed DP control of under-actuated vessels. Sørensen and Strand [6] proposed a DP control law for small-waterplane-area marine vessels like semisubmersibles with the inclusion of roll and pitch damping. Jensen [7] showed how proper modeling of pipe dynamics can be included in the DP guidance system. The DPS of semi-submersible drilling units has also been studied by Sun Liping [8], [9], Wang Lei et al. [10].

However, there are little papers doing research on the DPS during S-lay installation. In this paper, the time-domain simulation of DP during S-lay installation is obtained to draw some conclusions which will be useful for S-lay installation and the design of DPS. DPS is using the PID control in combination with Kalman filter. The SQP method is applied to get the optimal solution for the thrust allocation.

If your paper is intended for a *conference*, please contact your conference editor concerning acceptable word processor formats for your particular conference.

II. SYSTEM MODELING

A. Motion Equation

In general, ship's DPS is only concerned with low-frequency horizontal vessel motions (surge, sway, and yaw). However, the first-order motion, especially surge, heave and pitch, may affect the pipeline force on the vessel. So the motion equation of the vessel based on 3D radiation/diffraction theory can be given by:

$$(M + M_a) \ddot{x}(t) + C\dot{x}(t) + Kx(t) = F_{env} + F_{pipe} + F_{DP} \quad (1)$$

where M , M_a are the mass and add mass of the vessel, C is the damping matrix, F_{env} are the environmental loads, F_{pipe} is pipeline force on the vessel, F_{DP} are forces and moment delivered by the actuators unit.

B. Modeling of Dynamic Positioning System Plant Control

A nonlinear horizontal-plane positioning feedback controller of PID type is formulated as:

$$f(\varepsilon) = K_p \varepsilon + K_I \int \varepsilon dt + K_D d\varepsilon / dt + F_w \quad (2)$$

where K_p , K_I , K_D are the non-negative controller gain matrices, ε is the position and heading deviation vector, F_w is the wind feedforward force.

C. The Discrete-Time Kalman Filter for the Linear State Estimation Model

In the discrete-time case the dynamical system is assumed to be expressed in the form of a discrete-time state model:

$$\begin{cases} X(k+1) = \Phi X(k) + GU(k) + W(k) \\ Y(k) = CX(k) + V(k) \end{cases} \quad (3)$$

The kalman filter estimates the new state $\hat{X}(k+1)$ based on measurements and the previous state $\hat{X}(k)$, including two parts:

1. Time Update

$$P(k+1|k) = \phi P(k) \phi^T + R_1(k) \quad (4)$$

$$\hat{X}(k+1|k) = \phi \hat{X}(k) + \phi U(k) \quad (5)$$

2. Measurement Update

$$K(k+1) = P(k+1|k)C^T [CP(k+1|k)C^T + R_2(k+1)]^{-1} \quad (6)$$

$$P(k+1) = [I - K(k+1)C]P(k+1|k) \quad (7)$$

$$\hat{X}(k+1) = \hat{X}(k+1|k) \quad (8)$$

$$+ K(k+1)[Y(k+1) - C\hat{X}(k+1|k)]$$

where P is the estimation error covariance matrices associated with and K is the corrective term, Y is the output measurements, C is a positive definite matrix.

D. Thrust Allocation

The thrust allocation logic is responsible for delivering moment and forces calculated by control module algorithms. Such algorithms are oriented towards fuel consumption minimization. The sequential quadratic programming, described by [11], is applied into the optimal solution for the thrust allocation. The target function and constraint conditions can be written as follows:

$$f(x) = \min \left(\sum_{i=1}^N (x_{2i-1}^2 + x_{2i}^2) \right) \quad (9)$$

$$\text{s.t.} \begin{cases} f(\varepsilon) = \sqrt{x_{2i-1}^2 + x_{2i}^2} \\ T_{\max} \geq \sqrt{x_{2i-1}^2 + x_{2i}^2} \\ \alpha \geq \alpha_u \cup \alpha \leq \alpha_l \end{cases} \quad (10)$$

where x_{2i} , x_{2i-1} present the thrust in x and y direction, α , α_u , α_l are respectively thrust angle, upper ban angle and lower ban angel.

E. Coupling Model of Stinger and Pipe

The pipeline undergoing deep water S-lay installation contains three key regions. The first of these regions is known

as the overbend and it represents the upper part of the S-shape resting on the vessel and the stinger. The acting force between rollers of stinger and pipeline are simulated to the act between the U-type support as shown in Fig. 4 (b) and the pipeline by elastic surface contact [12], [13]. It is assumed that the acting force is only a braced force for the pipeline. Its stiffness can be obtained by [14]:

$$K_s = W_p / D \times 0.001 \quad (11)$$

where W_p is the distance between the two supporting point, D is the outer diameter of pipeline.

Then below the overbend there is a region of inflection after leaving the stinger, known as sagbend where the pipeline straightens out before its curvature is reversed to form the bottom region of the S-shape. Once the pipeline passes through the sagbend it finally reaches the relatively straight seabed region. The three regions of pipeline are calculated by lumped mass method. The effective tension T_e can be written as follow:

$$T_e = Q(\varepsilon) + (1 - 2\nu)P + eK_{nom}C / L_0 \quad (12)$$

where $Q(\varepsilon)$ is the function relating strain to wall tension, eK_{nom} is the axial stiffness at zero strain, C is the damping coefficient specified by critical damping value for a segment and target axial damping, L_0 is the unstretched length of segment, P is the pressure difference between the internal and external pressure, ν is the poisson ratio.

The bend moment of the pipeline is calculated by:

$$M = EI|C| + (\gamma_b / 100)D_{crit}w(C) \quad (13)$$

where EI is the bending stiffness, C is the curvature of the pipeline, γ_b is the target bending damping, D_{crit} is the bending critical damping value for a segment, $w(C)$ is the gradient of the curvature.

F. Simulation Process Model of the DPS

The process of the dynamic positioning during the S-lay installation is shown in Fig. 1.

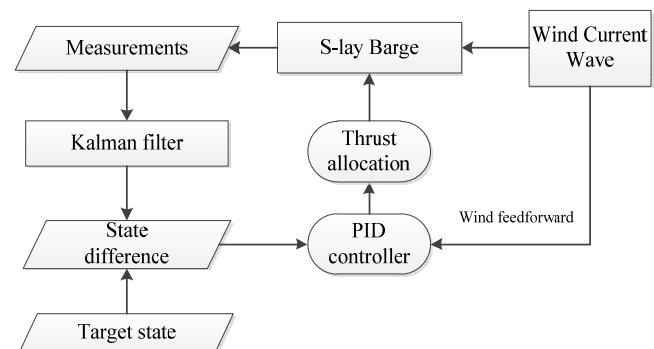


Fig. 1 Simulation process of dynamic positioning

III. NUMERICAL MODEL

The hydrodynamic model of the S-lay barge is shown in Fig. 2, and its main parameters are listed in Table I. The hydrodynamic model consists of 3459 surface elements and the stinger is simulated as Morrison rods. And then the added mass, damping, and RAO etc. are obtained through frequency-domain analysis of the model.

TABLE I
 PRINCIPLE OF THE HULL

Hull	LBP (m)	Breadth (m)	Depth (m)	Draft (m)	Roll (Kg*m ²)	Pitch (Kg*m ²)	Yaw (Kg*m ²)
10% S-lay	185	39.2	14	7.906	1.22e10	1.46e11	1.42e11

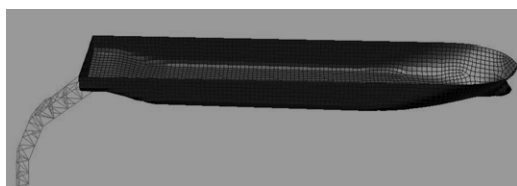


Fig. 2 Model of S-lay barge with stinger

The actuator unit consists of seven azimuth thrusters whose performance is listed in Table II, and arrangement is shown in Fig. 3.

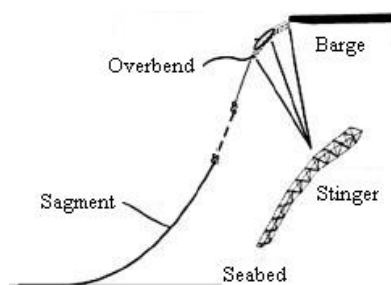


Fig. 3 The arrangement of thrusters

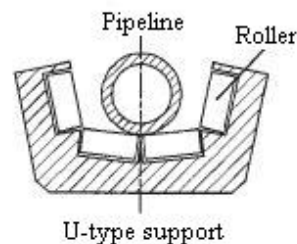
TABLE II
 PARAMETERS OF THE THRUSTER

Model	Propeller type	Dia (m)	Cather Angle (deg)	Max. Thrust (kN)	Max. Power (kW)	Rotation rate	Accommodation mode
Wartsila FS3500	4-bladed FPP	3.35	5	600	3500	181	RPM

The S-lay installation is illustrated in Fig. 4 (a), and Fig. 4 (b) shows the model of contact between the U-type supports and the pipeline. Besides, the tensioner which restrains the movement of the top of pipeline is carried out by using the fixed end constraint.



(a) S-lay installation



(b) Contact model

Fig. 4 Models of the vessel with pipeline and contact model of its roller

IV. RESULTS AND DISCUSSION

The wind force and moments are calculated by building block method, as specified by API. The wind is simulated as NPD wind spectrum, of which speed is 16m/s. The current force and moment are calculated by OCIMF, whose surface speed is 1.47m/s. The Jonswap wave spectrum is applied to simulate the wave load, whose Hs is 2.5m and T is 6.22s. The water depth is 1175m, and the length, outer diameter and thickness of pipeline are 2243m, 0.61m, 0.062m, respectively.

In this paper, five directions is designed for analysis, the direction is shown in Fig. 5. It is assumed that wind, current and wave load has the same direction.

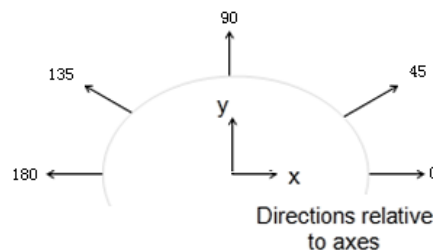


Fig. 5 Direction of environmental load

A. Influence of Wave Frequency Motion on Pipeline

In general, only low frequency motion is taken into account in DP. However, the force of pipeline acting on the barge is affected by surge, heave, and pitch. So the wave frequency motion should be in combination with low frequency motion. For the comparison between the low frequency motion only and the combination motion, the motion with wave frequency motion and without wave frequency motion was discussed as follows. The surge controlled by DP keeps a relatively constant value so that only the heave and pitch are the influence factors for the force of pipeline. Figs. 6 and 7 illustrate the great difference in heave and pitch between the low frequency motion and combination motion.

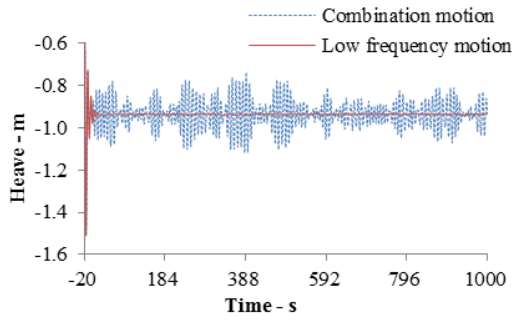


Fig. 6 Heave motion

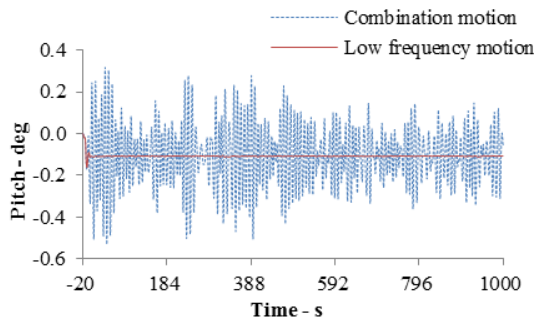


Fig. 7 Pitch motion

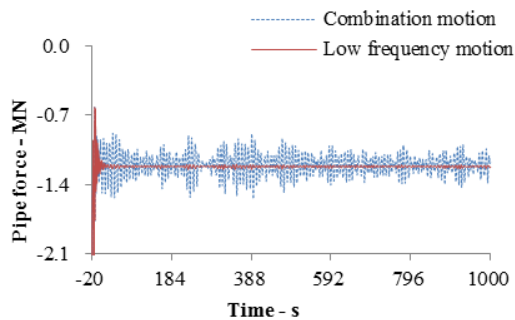


Fig. 8 Pipe force in x direction

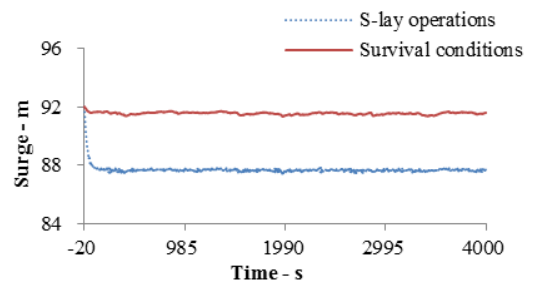
It can be seen in Fig. 8 that under the low frequency motion, the average force is -1215.215kN, the max is -1194.019kN, the min is -1246.257kN and the standard deviation is 8.19kN, while under the combination motion, the average force is -1209.65kN, the max is -896.657, the min is -1561.555kN and the standard deviation is 103.79kN. It can be concluded that during the simulation of DP during S-lay operations, the wave frequency, especially heave and pitch, should be taken significantly into account.

Another comparison between wave frequency motion without pitch and wave frequency motion without heave has also been discussed in this paper. Under the motion without pitch, the average pipe force in x direction is -1214.95kN, the max is -1168.43kN, the min is -1260.92kN and the standard deviation is 14.62kN. Meanwhile, under the motion without heave, the average force is -1211.33kN, the max is -952.28kN, the min is -1518.22kN and the standard deviation is 88.74kN. So it can be concluded that heave accounts for nearly 85% while pitch accounts for 15% in the variation of pipe force in x

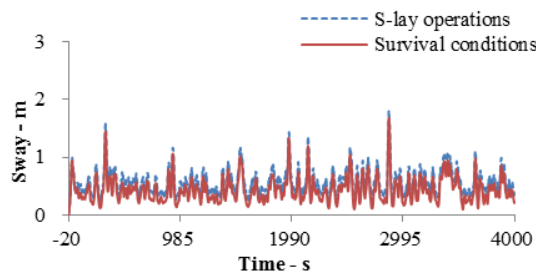
direction. The reason is that the heave only caused the pipeline moving in z direction whereas the pitch caused the great increase and decrease in the horizontal component of axial tension of the pipeline.

B. Time-Domain Simulation of DP during S-Lay Installation Coupling Effect of Stinger-Pipeline-Barge on Positioning Accuracy

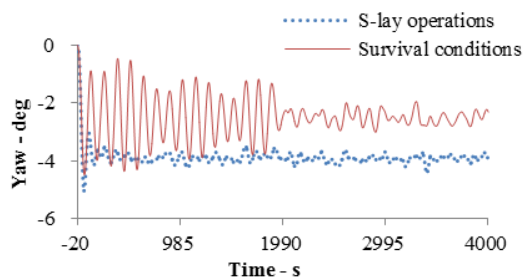
To study the coupling effect of stinger-pipeline-barge on positioning accuracy, two cases, S-lay operations and survival conditions, were set as model controls. And the direction of environmental load was selected to be 135°. The target position was set as $X=92m$, $Y=0m$, $Yaw=0^\circ$. Fig. 9 reveals the surge, sway and yaw time history in two cases. Comparing the changes of sway shown in Fig. 9 (b), ones can find that the surge and yaw have greater amplitude changes.



(a) Surge motion



(b) Sway motion



(c) Yaw motion

Fig. 9 Horizontal motion of S-lay barge

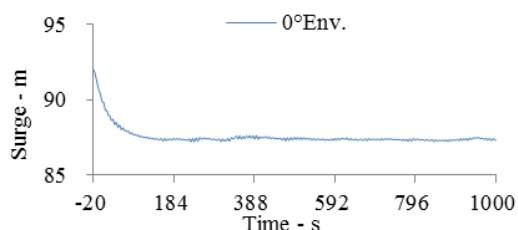
TABLE III
THE STATISTICS OF THE S-LAY BARGE HORIZONTAL MOTION

Case	Motion	Min.	Max.	Average	Standard deviation
S-lay operations	Surge(m)	87.43	87.86	87.67	0.06
	Sway(m)	0.23	1.82	0.58	0.23
	Yaw(deg)	-4.41	-3.60	-3.91	0.12
Survival conditions	Surge(m)	91.18	91.68	91.25	0.08
	Sway(m)	0.09	1.68	0.454	0.23
	Yaw(deg)	-3.00	-1.94	-2.50	0.22

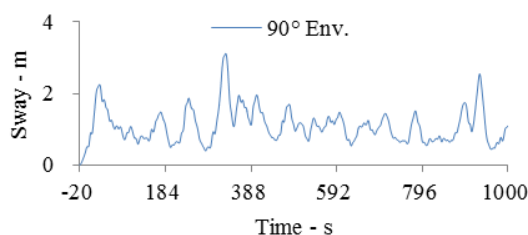
The result comparison between two cases is given in Table III. Because of the axial tension of pipeline, the surge amplitude under S-lay operations is 5.79 times larger than that under survival conditions. Meanwhile, the sway and yaw amplitude under S-lay operations also get 1.29 times and 1.56 times larger than ones under survival conditions due to the transverse force and yaw moment caused by the elastic contact between the pipeline and U-type rollers. Besides, it can be seen from the deviation listed in Table III that the motion of barge under S-lay operations is relatively steady compared with motion under survival conditions, especially in surge and yaw.

C. Time-Domain Simulation of Dynamic Positioning under Different Circumstances during S-Lay Installation

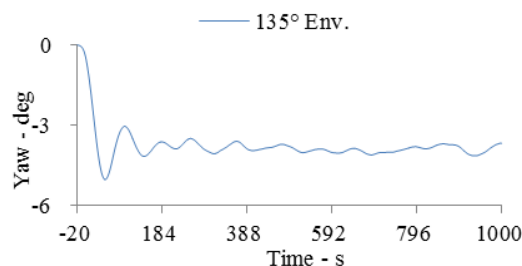
The maximal offset relative to destination location is an important factor. Thereby the surge, sway and yaw offset in different environment load directions are shown in Fig. 10. Table IV lists the statistics of the S-lay barge horizontal motion in pipe-laying condition. The time is from 150s to 1000s.



(a) Surge motion



(b) Sway motion



(c) Yaw motion

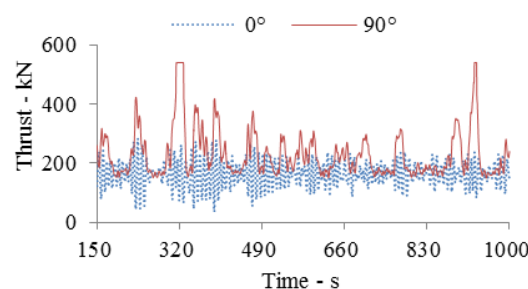
Fig. 10 Motion of S-lay barge

TABLE IV
THE STATISTICS OF THE S-LAY BARGE HORIZONTAL MOTION

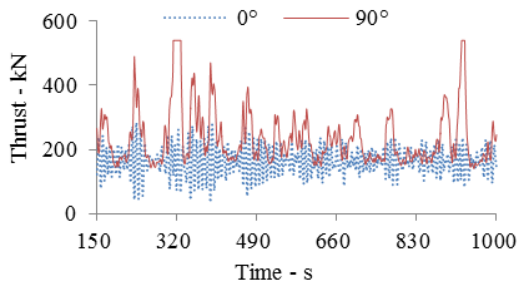
Load direction	Horizontal motion	Minimum	Maximum	Average	Standard deviation
0°	surge(m)	87.19	87.60	87.37	0.07
	sway(m)	0.06	0.06	0.06	0.00
	yaw(deg)	-0.01	-0.01	-0.01	0.00
45°	surge(m)	87.29	87.79	87.48	0.09
	sway(m)	0.27	1.38	0.55	0.19
	yaw(deg)	1.20	2.25	1.75	0.23
90°	surge(m)	87.54	87.70	87.60	0.03
	sway(m)	0.39	3.12	2.11	0.48
	yaw(deg)	-2.66	-2.10	-2.34	0.11
135°	surge(m)	87.47	87.82	87.68	0.07
	sway(m)	0.23	1.58	0.55	0.07
	yaw(deg)	-3.85	-3.49	-3.68	0.14
180°	surge(m)	87.66	87.95	87.82	0.05
	sway(m)	0.06	0.06	0.06	0.00
	yaw(deg)	-0.01	0.00	-0.00	0.00

According to the statistics in Table IV, when the barge lays pipe in 0° load direction, the pitch motion becomes fiercer (Fig. 15) and has great influence on axial pipe tension (Fig. 16). Thus surge motion has the -4.81m maximum offset. As the longitudinal projected area is larger, the maximum sway motion is 3.12m in 90° load direction. In addition, the maximum yaw motion is -3.87° in 135° load direction considering the force on superstructure. It also can be concluded that the dynamic positioning system has a good positioning accuracy and can meet positioning requirements [15].

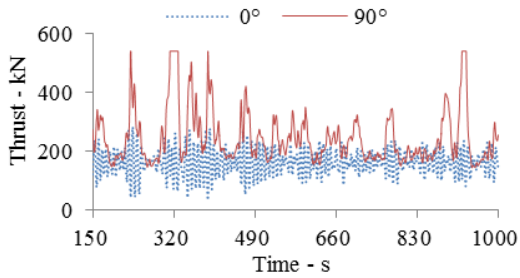
Thrust force allocation principle is ensuring minimal power consumption. Fig. 10 describes the force curve of the thrusts in 0° and 90° load direction. 1#, 2#, 4# and 6# thrust is shown considering the symmetry.



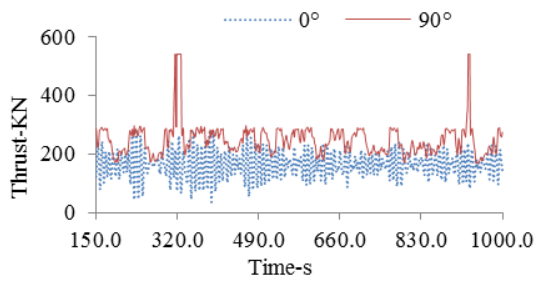
(a) 1#thrust force



(b) 2#thruster force



(c) 4#thruster force



(d) 6#thruster force

Fig. 11 The force of thrusters

It can be seen from Fig. 11, the thrusters force varies steadily in specified bounds and the power consumption is relatively small in 0° load direction. As the longitudinal projected area is larger, the thruster force changes obviously and can reach upper limit value 540kN in 90° load direction. Lateral environment loads should be avoided in pipe-laying. The total power changing over time is shown as Fig. 12. Fig. 13 illustrates power consumption of dynamic positioning system in every environment load directions.

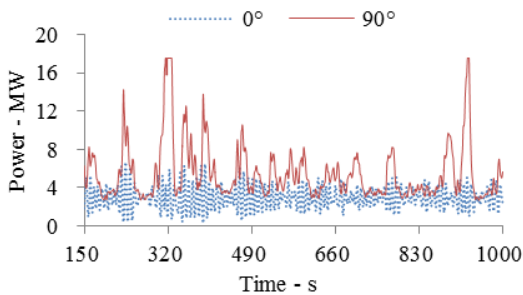


Fig. 12 The total power

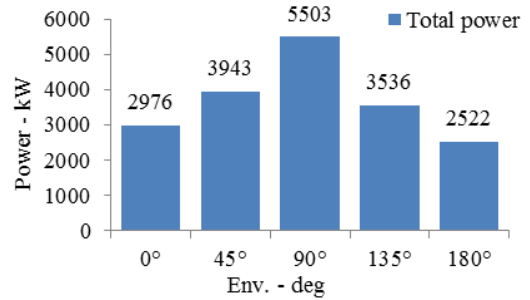


Fig. 13 The power consumption of dynamic positioning

As can be seen from the above diagram, pipe laying barge works in head sea, the dynamic positioning system gets the minimum power consumption 2522kW, reduces about 50% than in 90° load direction. There also has been some difference between power consumption in 0° and 180° load direction. The main factor is the pipe force acting on the hull. In order to find the reason, it is necessary to analyze the heave and surge motion of the barge and the pipe force in x direction.

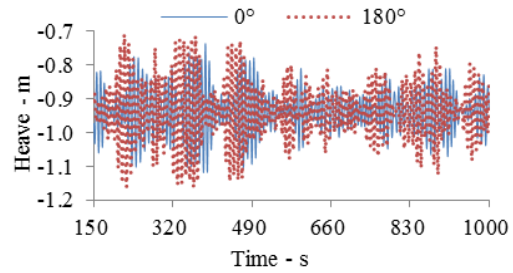


Fig. 14 Heave motion

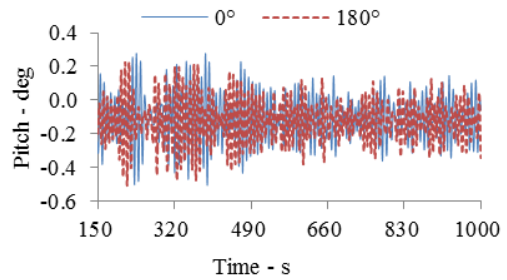


Fig. 15 Pitch motion

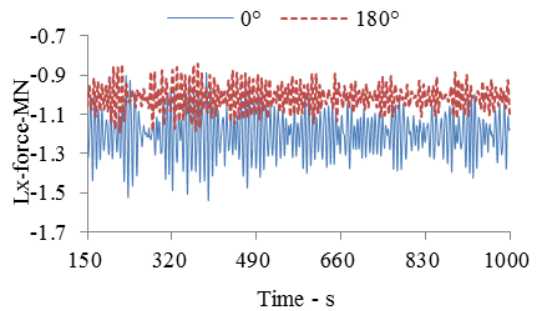


Fig. 16 Pipe force in x direction

From the above curves, in 0° load direction, the mean value of pipe force on the hull is -1196.94kN, the standard deviation of pitch motion is 0.134 deg, the standard deviation of heave motion is 0.064m. In 180° load direction, the mean value of pipe force on the hull is -1014.06kN, the standard deviation of pitch motion is 0.125°, the standard deviation of heave motion 0.080m. It shows that the main effect of wave frequency motion on pipe force is pitch motion.

D. Pipe Line Stress Check

According to criterion API RP 2RD [16] the von-Mises stress of conventional steel cylinder pipe, +API can be expressed as follow.

$$\sigma_{API} = 0.5\sqrt{(\sigma_{p\theta} - \sigma_{pz})^2 + (\sigma_{pz} - \sigma_{pr})^2 + (\delta_{pr} - \delta_{p\theta})^2} \quad (14)$$

where

$$\begin{aligned} \delta_{pr} &= -(P_0 D_0 + P_I D_I) / (D_0 + D_I), \\ \sigma_{p\theta} &= (P_I - P_0) D_0 / 2t - P_I, \\ \sigma_{pz} &= T / A \pm M (D_0 - t) / 2I \end{aligned}$$

P_I is pipe internal pressure, P_0 is pipe external pressure, D_I and D_0 is inside and outside diameter of pipe, t is pipe wall thickness, A is cross-sectional area of pipe wall, T is pipe wall tension, M is global bending moment, I is inertia moment.

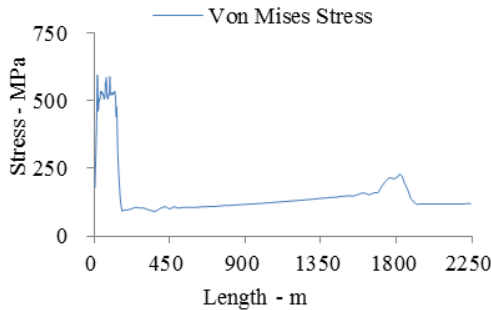


Fig. 17 Curve of pipe maximum stress checking

For S-lay installation, bending stress of conventional steel pipe can be calculated by the following expression [17].

$$\delta_a = \frac{ED}{2R_{cv}} \quad (15)$$

where, δ_a is bending stress of bending segment; E is modulus of elasticity, D is outside diameter of pipe, R_{cv} is curvature radius of stinger.

The results show that bending stress of bending segment is 554.55MPa, differs by 5.4% from the maximum stress in Fig 16. This demonstrates that the simulation of pipe-stinger coupling is reasonable and the results are available.

V. CONCLUSIONS

A time domain analysis of dynamic positioning system has been developed combined with positioning control system consisted of PID and Kalman filtering and thruster force allocation system with minimum power consumption. And the wave frequency motion effect is analyzed on pipe-stinger coupling force. Positioning accuracy change, thruster force allocation and power consumption is analyzed in pipe-laying condition. The conclusions are shown as follows.

- 1) Wave frequency motion has a great influence on pipe force and dynamic positioning system. And for the dynamic positioning system, the wave frequency motion in surge accounts for about 85% of the force and heave accounts for about 15% of the force.
- 2) In pipe-laying condition, the dynamic positioning accuracy decreases obviously which is reflected in the motion amplitude in surge and yaw increasing. And the variance of surge and yaw motion is less in pipe-laying condition.
- 3) Pipe-laying in head sea is the optimum laying way of all the environment loadings. It withstands less environment loadings and less pipe axial stress. And dynamic positioning system has minimum power consumption and optimal positioning accuracy in head sea. It is really an important way that decreasing pitch motion and pipe-laying in head sea to ensure pipe-laying and dynamic positioning system safety.

ACKNOWLEDGMENT

This paper is funded by the International Exchange Program of Harbin Engineering University for Innovation-oriented Talents Cultivation.

REFERENCES

- [1] Fay, H., "Dynamic Positioning System: Principles, Design, and Application(J)". Editions Technip, Paris, 1990.
- [2] Ayman B. Mahfouz, Hussein W. El-Tahan. *Ocean Engineering*, June 2006, pp.1070-1089
- [3] Haibo Chen, Torgeir Moan. *Reliability Engineering & System Safety*, July 2008, pp.1072-1090
- [4] Haibo Chen, Torgeir Moan, *Reliability Engineering & System Safety*, Volume 84, Issue 2, May 2004, pp.169-186
- [5] K.Y. Pettersen, F. Mazenc, H. Nijmeijer. "Global uniform asymptotic stabilization of an underactuated surface vessel: Experimental results(C)". *IEEE Transaction on Control System Technology*, 2004, pp.891-903
- [6] A.J. Sørensen, J.P. Strand. "Positioning of small-waterplane-area marine constructions with roll and pitch damping(J)". *Control Engineering Practice*, 2000, pp.205-213
- [7] Jensen, G. A. "A nonlinear PDE formulation for offshore vessel pipeline installation(J)". *Ocean Engineering*, 2010, pp. 365-377
- [8] Fang Wang, Liping Sun. "Modeling and Simulation of Dynamic Positioning Deepwater Semi-submersible Drilling Units(J)". *Ship Engineering*, 2011, pp.75-78
- [9] Liping Sun, Jing Chen. "Time domain simulation of a semi-submersible platform with thrusters failed in dynamic positioning(J)". *The Ocean Engineering*, 2013, pp.38-44
- [10] Wang L, Sun Pan. "Research on time domain simulation of dynamic positioning for a deep water semi-submersible platform(J)". *Scientia Sinica*, 2011, pp.123-131
- [11] Qing Ni, "Optimization algorithm and programing(M)", Science press, Beijing, 2009.
- [12] Silva D M L, Jacob B P. "A contact model for the simulation of line collision in offshore oil exploitation (C)". *Proceedings of the XXVIII*

Latin American Congress on Computational Methods in Engineering
Porto, Portugal, 2007, pp.22-35

- [13] Silva D M L, Jacob B P. "A generalized contact model for nonlinear dynamic analysis of floating off-shore systems (C)". Proceedings of the 25th International Conference on Offshore Mechanics and Arctic Engineering Hamburg, Germany, 2006, pp.92-155
- [14] Gong S F, Chen K, Chen Y, et al. "Configuration analysis of deep water S-lay pipeline (J)". China Ocean Engineering, 2011, vol 25(3): pp.519-530.
- [15] Asgeir J.Sorensen, Bernt Leira, Jann Peter Strand. "Optimal set point chasing in dynamic positioning of deep-water drilling and intervention vessels (J)", Int.J.Robust Nonlinear Control, 2001, pp.1187-1205.
- [16] API. Design of risers for floating production systems and TLPs(S), 2006, 5(2):pp.53-54.
- [17] BoyunGuo, Shanhong Song, Ali Ghalambor, Tian Ran Lin. Offshore pipelines(2nd Edition) (M), 2014, pp.13-20